

Chapter VIII

A comparative study of targeting
nanoparticle–drug complexes to tumor by
magnetic field and hypoxic cell sensitizer

Chapter VIII: A comparative study of targeting nanoparticle-drug complexes to tumor by magnetic field and hypoxic cell sensitizer

Table of Contents

- 8.1 Introduction**
- 8.2 Materials and Methods**
 - 8.2.1 *Animals*
 - 8.2.2 *Chemicals*
 - 8.2.3 *Preparation of nanoparticles and its characterization*
 - 8.2.4 *Experimental design*
 - 8.2.5 *Tumor regression study*
 - 8.2.6 *The cellular DNA damage analysis*
 - 8.2.7 *RNA isolation, cDNA synthesis and PCR*
 - 8.2.8 *Serum biochemical analysis*
 - 8.2.9 *Ferrozine assay*
 - 8.2.10 *Histopathology*
 - 8.2.11 *Statistical analysis*
- 8.3 Results and Discussion**
 - 8.3.1 *Analysis on Tumor regression*
 - 8.3.2 *Cellular DNA damage analysis*
 - 8.3.3 *Assessment on iron content in tumor and liver tissues*
 - 8.3.4 *Transcriptional expression of genes responsible for tumor growth and cell death*
 - 8.3.5 *Analysis on the morphology of tumor tissues*
 - 8.3.6 *Assessment on serum biochemical parameters*
- 8.4 Conclusion**

In our previous studies, we reported the effect of specific delivery of cytotoxic drug, Berberine (BBN) to tumor in association with magnetic iron-oxide nanoparticles (NP) by physical (using an external magnetic field) and chemical (using hypoxic cell sensitizer Sanazole (SAN)) methods. In the present work, a comparison has been made between both targeting methods in solid tumor-bearing animals. The comparative study in tumor regression and the underlying mechanism were performed in order to compare the efficacy of both methods for tumors of identical origin and similar conditions. The tumors were found to be reduced in both treatments. The more iron content in tumor tissues of NP-BBN-SAN group in comparison with NP-BBN-Magnet revealed the higher accumulation of these complexes in tumors. The results from gene expression studies by PCR, analysis on tumor morphology and serum biochemical parameters further confirms the therapeutic potential of both targeting strategies in tumor control. However, the magnetic field directed tumor therapy has some limitations as this strategy is restricted to magnetic nanoparticles and tumors in the periphery of the body, not located in depth. Further studies on these treatment strategies are worthwhile to be taken up.

8.1 INTRODUCTION

Targeted delivery of therapeutic agents specifically to tumor can maximize the success of tumor therapy by achieving higher drug concentration in the tumor and lack of systemic toxicity and side effects. Different strategies have been used for targeted delivery, such as physical, chemical and biological methods. Use of nano-sized particles revolutionized targeted tumor therapy, since these particles can accumulate in tumor, by exploring alterations in the tumor vasculature, known as the enhanced permeability and retention effect [Greish, 2007].

Magnetic nanoparticles (iron-oxide) have attained importance in this regard as these particles are biocompatible and can manipulate them to specific sites by the application of an external magnetic field. Magnetic nanoparticles of size 10-100nm are found to have relevance in drug targeting. The particles with size >150nm are taken up differently through macrophage activation. The deleterious effects of conventional chemotherapeutics can be avoided by magnetic field directed targeting of their conjugates with iron-oxide nanoparticles. Several preclinical and clinical trials on targeting of chemotherapeutic drug Doxorubicin have been reported to increase the therapeutic efficacy by enhancing specificity, and preventing non-specific action and associated systemic toxicities especially cardiotoxicity [Goodwin et al., 2001; Koda et al., 2002; Wilson et al., 2004].

In our previous studies, we reported that physical targeting by the application of an external magnetic field [Sreeja and Nair, 2015; Jayakumar et al., 2009] and chemical targeting using a hypoxic cell sensitizer, Sanazole, was effective to specifically deliver the complexes of magnetic iron-oxide nanoparticle (NP) and drugs (BBN and DOX), leading to tumor regression. In the present study, we tried to make a comparison between magnetic field directed and sanazole directed targeting of NP-BBN complexes.

8.2 MATERIALS AND METHODS

8.2.1 *Animals*

Female *Swiss albino* mice weighing 25 - 29 g obtained from the Small Animal Breeding Section (SABS), Mannuthy, Thrissur, Kerala were kept under standard conditions in the Centre's Animal House Facility. All animal experiments in this study were carried out with the prior approval of the Institutional Animal Ethics Committee (IAEC) and were conducted strictly adhering to the guidelines of CPCSEA constituted by the Animal Welfare Division of Government of India.

8.2.2 *Chemicals*

Berberine chloride, Iron (III) chloride, Iron (II) chloride and Ammonium hydroxide solution were purchased from Sigma chemical company, India. All other reagents were of analytical grade and procured from reputed Indian manufacturers.

8.2.3 *Preparation of nanoparticles and its characterization*

The NPs were prepared by co-precipitation method [Sophie et al., 2008]. The surface of the nanoparticles was modified by coating with POES; complexed with drugs -BBN and SAN- by sonochemical method and these nano-drug complexes were characterized by FTIR, XRD and TEM as reported in the previous chapters.

8.2.4 *Experimental design*

Tumor was developed on the hind limb of the animals by transplanting DLA cells (1×10^6 cells in 100 μ l), subcutaneously. Fourteen days after transplantation, the tumor-bearing animals were divided into five groups with five animals in each group as described below.

Group 1: Control- untreated tumor- bearing animals

Group 2: NP-BBN-Magnet (animals treated with NP-BBN complexes and directed by a magnetic field); 100mg/kg

Group 3: NP-BBN-SAN (animals treated with NP-BBN-SAN complexes); 20mg/kg
The animals were administered with NP-drug complexes for seven consecutive days.

8.2.5 *Tumor regression study*

The thickness of hind limb was measured using Vernier calliper every 3rd day during administration. Tumor volume was calculated (Divakaran et al., 2001) as follows,

Tumor radius = radius of tumor-bearing hind limb – radius of normal hind limb

Tumor volume = $\frac{4}{3}\pi r^3$ where 'r' is the radius.

8.2.6 *The cellular DNA damage analysis*

Alkaline single cell gel electrophoresis (Comet assay) was performed to assess the extent of damage to cellular DNA. The cells were embedded on slides pre-coated with 1% normal agarose. The cellular membranes were lysed by incubating cells in lysis solution. Finally, electrophoresis was carried out for 30 min at 20V [Nair and Nair, 2011].

8.2.7 *RNA isolation, cDNA synthesis and PCR*

RNA was isolated from tumor tissues of animals in the study group by acid guanidium thiocyanate-phenol-chloroform extraction method [Chomczynski and Sacchi, 2006]. Reverse transcription was done on the isolated RNA with random primer to obtain cDNA. PCR was done on the cDNA using primers specific for various genes. The expression of genes *-bax*, *bcl2* and *β -actin* was studied by conventional PCR (RT-PCR) and the expressions of genes *-hif-1 α* , *bax*, *akt*, *caspase 8* and *caspase 9* were studied by real time PCR. The cycling conditions were depicted in chapter II.

8.2.8 *Serum biochemical analysis*

Serum urea level was studied by Diacetyl monoxime (DAM) reagent method [Kassirer, 1971], SGPT [Winkelman et al., 1974], Bilirubin [Gornall et al., 1949] and total protein [Walter, 1980] were also analysed (Agappe Diagnostic Pvt. Ltd.; Ernakulam, Kerala, India).

8.2.9 *Ferrozine assay*

The concentration of iron in tissues was analyzed by direct specific determination of Iron in tissue samples using ferrozine. The iron gets reduced at pH 1.7 by treating with 10g/L ascorbic acid solution in 0.1mol/L HCl. The reduced iron reacts with ferrozine to produce

a coloured product, at higher pH, having absorption maximum at 570nm [Rierner et al., 2004].

8.2.10 *Histopathology*

The alterations in tumour and liver tissues following the treatments were visualized by histopathology analysis. The tissues were fixed in formalin and impregnated with wax. Small sections taken from the tissue blocks were stained by hematoxylin-Eosin staining method [Culling, 1974].

8.2.11 *Statistical analysis*

The results are presented as Mean \pm SD. Statistical analyses of the results were performed using ANOVA with Tukey-Kramer multiple comparisons test.

8.3 RESULTS AND DISCUSSION

8.3.1 *Analysis on Tumor regression*

The tumor-bearing animals were administered with the nano-complexes and tumor volume was measured on every 3rd day for a period of twelve days. The reduction in tumor volume was observed in animals treated with NP-BBN-SAN complexes and NP-BBN complexes along with the application of an external magnetic field compared to the untreated control as presented in figure 8.1.

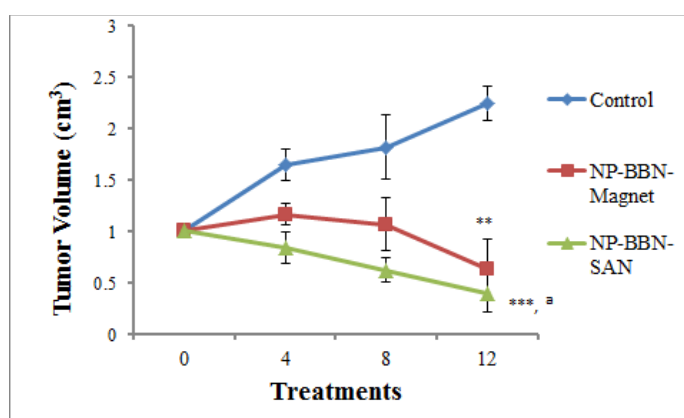


Figure 8.1: Tumor volume following various treatments. Note: The values are presented as mean \pm SD. The significance with p value <0.001 and <0.01 were observed in NP-BBN-SAN group and NP-BBN-Magnet in comparison with the control (untreated) and ‘a’ indicates non-significance with respect to NP-BBN-Magnet.

8.3.2 Cellular DNA damage analysis

The comet assay was used to analyse damage in the cellular DNA (figure 8.2). Comet shaped cells, as an indicator of cellular DNA damage, were observed in the tumor tissue of the treatment groups. However, there were no such changes noticed in the blood cells and liver tissues of control and treated groups. The results suggested that these treatments are effective in inducing cellular DNA damage in tumor tissue without causing any changes to normal cells in the body.

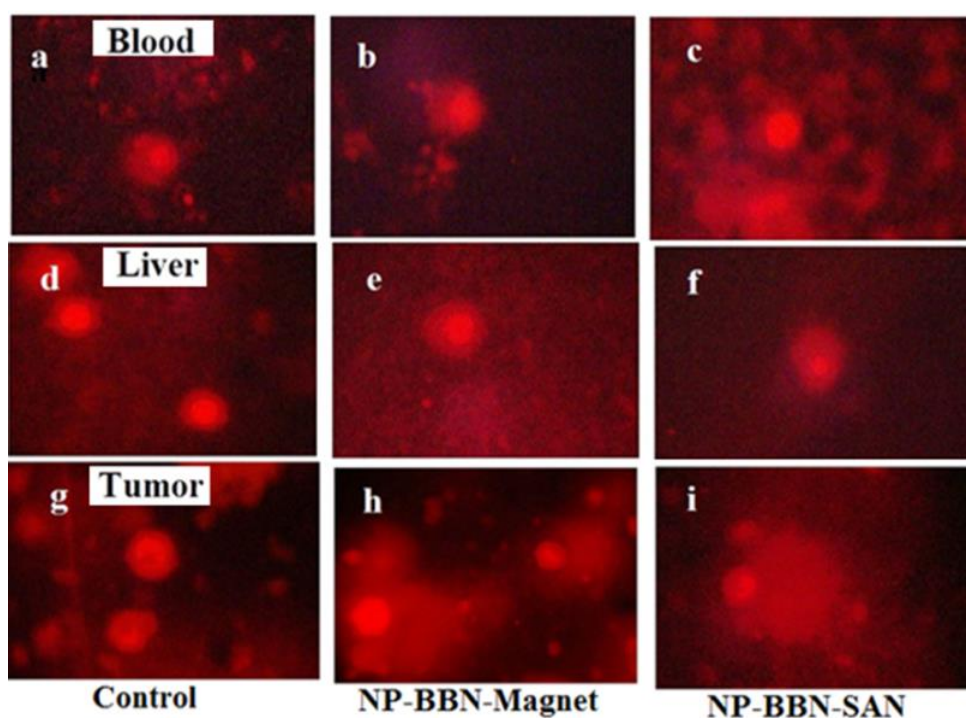


Figure 8.2: Images of cells (blood, liver and tumor) after alkaline single cell gel electrophoresis.

8.3.3 Assessment on iron content in tumor and liver tissues

Iron content in tumor and liver tissues was analysed by ferrozine assay as presented in figure 8.3. The concentration of iron in tumor following both treatments was significantly increased from control however; a greater variation can be seen in NP-BBN-SAN treated group, suggesting the higher accumulation of the complexes in tumor. In this group there was a slight increase in the iron concentration in the liver which could be due to the liver-mediated detoxification process.

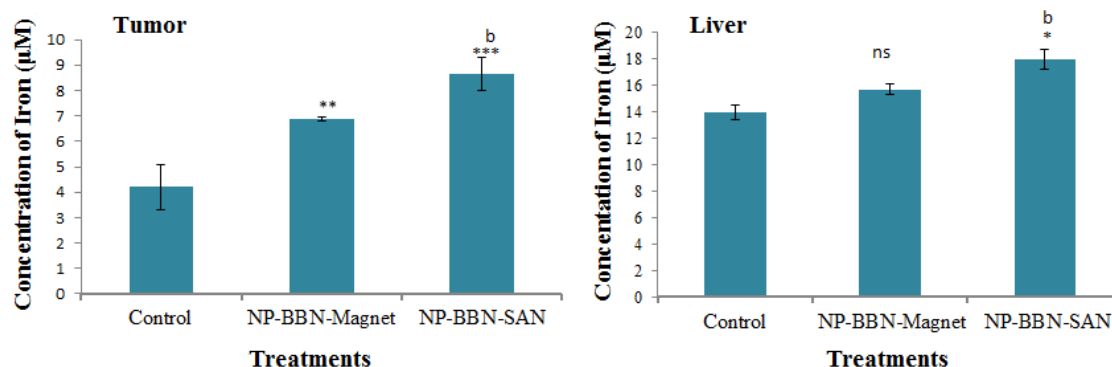


Figure 8.3: Concentration of iron in tumor and liver tissues. Note: The values are presented as mean± SD. ‘ns’ indicates non-significance ($p>0.05$); ‘*’ ‘**’ ‘***’ indicates significance with p value <0.05 , <0.01 and <0.001 respectively when compared to the control as well as ‘b’ indicates significance ($p<0.01$) with respect to NP-BBN-Magnet.

8.3.4 *Transcriptional expression of genes responsible for tumor growth and cell death*

The transcription of genes- *bax* and *bcl2* - was studied by RT-PCR and the gel images were presented in figure 8.4(I). The *bax* to *bcl2* ratio (figure 8.4II) was calculated and presented in figure 8.4(II). The ratio, *bax* to *bcl2*, is an indicator of apoptosis [Chen et al. 2002]. The higher *bax* to *bcl2* ratio seen in the figure is indicative of apoptosis as the major mechanism of induction of cell death in both treatments.

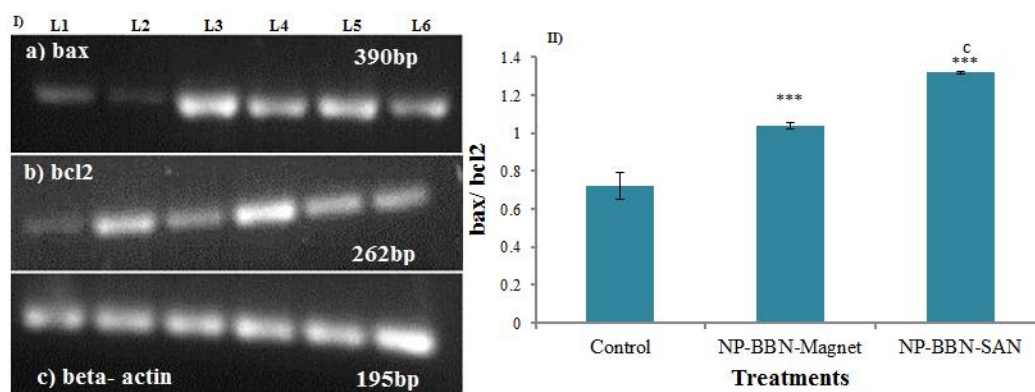


Figure 8.4: I: Gel images after PCR and II: *bax*-*bcl2* ratio. Note: The values are presented as mean±SD. ‘***’ indicates significance with p value <0.001 when compared to the control as well as ‘c’ indicates significance ($p<0.01$) with respect to NP-BBN-Magnet.

The relative fold change in the transcription of genes was studied by qRT-PCR and the results were shown in figure 8.5. The transcription of *hif-1 α* , major factor responsible for hypoxic tumor progression [Semenza, 2000 and 2001], was down regulated in both

physical- magnetic field directed- and chemical- SAN directed- treatments in comparison with the controls.

The gene *akt* was down regulated 1.2 fold following NP-BBN-Magnet ($p < 0.01$) treatment while there was six fold down regulation ($p < 0.001$) of this gene in NP-BBN-SAN treatment with respect to the control. The expression of *akt* contributes to tumor metastasis via activating matrix metalloproteinases (Thant et al., 2000). As metalloproteinases are involved in metastasis, these treatments would have inhibitory effect on tumor metastasis.

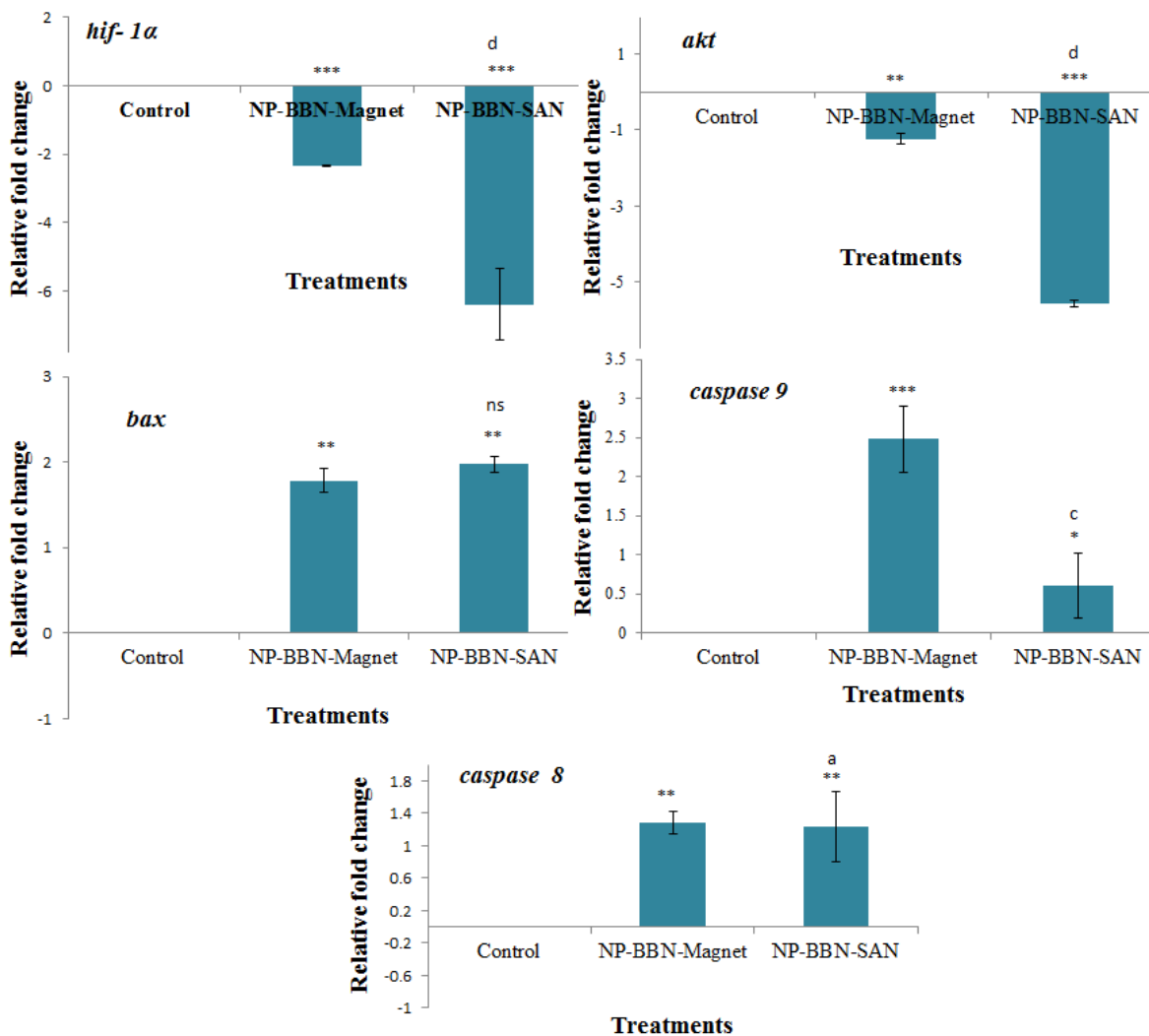


Figure 8.5: Relative fold change in the transcription of genes- *hif-1α*, *akt*, *bax*, *caspase 8* and *caspase 9*. Note: The values are presented as mean± SD. ‘*’, ‘**’, ‘***’ indicates significance with p value <0.05, <0.01 and <0.001 respectively when compared to the control. ‘ns’ indicates non-significance ($p > 0.05$) and ‘b’ indicates significance ($p < 0.01$) with respect to NP-BBN-Magnet.

The apoptotic gene *bax* expression was up regulated significantly in both treatments ($p < 0.01$) compared to the control. The transcription of enzymes *caspase 9* and *caspase 8* was found increased significantly in both cases. The expression of *caspase 9* was to a greater extent in NP-BBN-Magnet treatment than in the case of NP-BBN-SAN treatment. The gene *caspase 8* was up regulated in the same extent in both treatment methods. These results suggest that both intrinsic and extrinsic pathways are operative in both the treatment cases while intrinsic pathway could be more prominent in NP-BBN-Magnet treatment and extrinsic pathway in NP-BBN-SAN treated group.

8.3.5 Analysis on the morphology of tumor tissues

Histopathological studies showed no morphological alterations in liver tissue (figure 8.6) following both the treatments. Thus, these treatments have no adverse effects on liver. However, histopathological studies showed severe morphological alterations in the tumor tissue following the treatments as discernible from the figure 8.7. Necrotic and apoptotic areas are evident in the figures 8.7b and c.

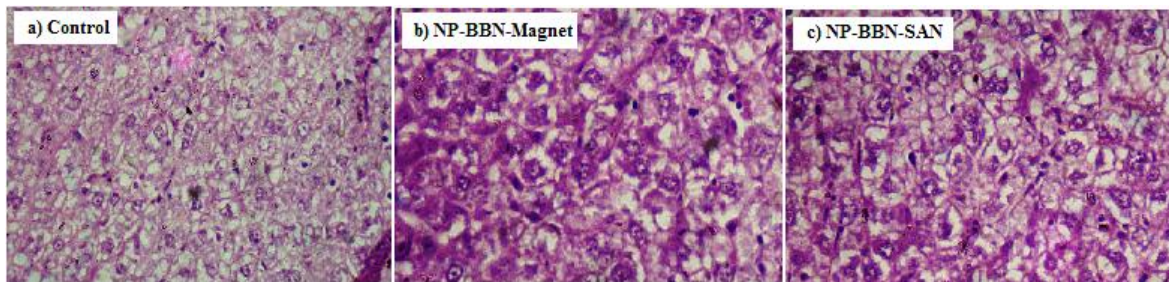


Figure 8.6: Morphology of liver - a) Control, b) NP-BBN-Magnet and c) NP-BBN-SAN.

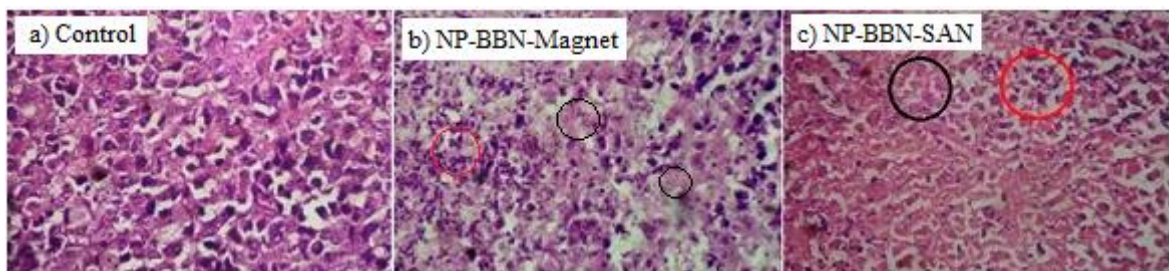


Figure 8.7: Morphology of tumor - a) Control, b) NP-BBN-Magnet and c) NP-BBN-SAN. The necrotic cells are marked with black circle and cells with condensed/fragmented nuclei are marked with red circle.

8.3.6 Assessment on serum biochemical parameters

The serum parameters- urea, albumin, SGPT and total protein- were also determined and found that all values are in normal range (table 8.1). This would indicate that the treatments cause tumor specific damage, sparing normal tissues- liver and kidney.

Table 8.1: Serum biochemical parameters following various treatments

| Treatments | Urea (mg/dl) | SGPT (U/L) | Albumin (g/dl) | Total protein (g/dl) |
|-------------------|---------------------|-------------------------|-----------------------|-----------------------------|
| Control | 41.3±0.2 | 57.7±21.3 | 2.3±0.25 | 2.47±0.01 |
| NP-BBN-Magnet | 35.4±2.9* | 66.4±0.14 ^{ns} | 1.7±0.12* | 2.14±0.03 ^{ns} |
| NP-BBN-SAN | 25.2±1.9** | 47.9±3.4** | 1.7±0.1* | 3.035±0.13* |

Note: The values are presented as mean± SD. ‘ns’ indicates non-significance (p>0.05), ‘*’ and ‘**’ indicates significance with p<0.05 and <0.01 respectively when compared to the control.

8.4 CONCLUSION

The present study revealed that the two methods - physical method using external magnetic field and chemical method using SAN - were found effective in targeting of NP-BBN complexes to tumor. However, the physical method of targeting using magnetic nanoparticles and external magnetic field may not be suitable for deep-seated tumors. The present study demonstrated tumor regression in case of peripheral tumors. Chemical targeting of nano-drug complexes with SAN would be effective to treat tumors located in depth as well as peripheral. However, more studies are needed to demonstrate the effect of chemical targeting of nanoparticles in deep-seated tumors. Further, the physical method of magnetic field directed targeting limits the use to magnetic nanoparticles only, while in case of chemical method nanoparticles can be magnetic as well as non-magnetic.